

The Ex Vivo Pig Eye as a Replacement Model for Laser Safety Testing

James G. Fyffe,¹ Thomas A. Neal,¹ William P. Butler,¹ and Thomas E. Johnson^{2,*}

The purpose of this study was to evaluate the viability of ex vivo pig eyes as a replacement model for in vivo testing in the establishment of laser eye safety standards. Previous studies of pulsed energy absorption at 3.8 μm were performed using rhesus monkey cornea at pulse durations two orders of magnitude shorter than the 8- μs pulses used in the current study. Ex vivo pig eyes were exposed to laser pulses of various energies and then evaluated to establish the statistical threshold for corneal damage. Tissue analysis (histologic evaluation) was used to determine the extent of damage to the cornea. These results can be used in the establishment of safety standards for laser use; our findings also suggest that ex vivo pig eyes are suitable models for this purpose.

One of the most impressive tools in medicine, science, and technology today is the laser (light amplification by stimulated emission of radiation). Since the first laser system was built in 1960, applications of this technology have expanded rapidly. For example, the laser became a widely used tool in the field of surgery by the mid-1980s (26). With the increasing use of lasers and laser systems, it is necessary to assess the health effects and hazards of nonionizing laser radiation. The American National Safety Institute (ANSI) currently sets laser safety standards in the United States. Because of the nature and technological advancements of nonionizing radiation laser systems (adjustable wavelengths, frequencies, etc.), one exposure standard for all laser systems may not ensure adequate protection. Generally, safety standards are based upon empirical data collected from sources such as medical reports and experimental investigations. In some cases, safety standards have been extrapolated from other studies (e.g., infrared data).

Each wavelength of laser radiation is absorbed, reflected, or transmitted differently by tissue. Regarding laser safety, exposure limits are grouped into three basic categories according to wavelength: ultraviolet (0.2 to 0.4 μm), visible (0.4 to 0.7 μm), and infrared (IR; 0.7 to 10 μm). Understanding the nature of damage to tissues involves multiple parameters that include wavelength, fluence (energy per unit area), and power (the rate at which energy is delivered to the area; 5). Although the laser-tissue interaction is multifactorial and complex, objective measures such as the aversion response time (the maximal amount of time that laser radiation can be focused in one spot before causing damage) generally are helpful tools in assessing damage to tissue (in this experiment, corneal damage). For example, the aversion response time for continuous wave lasers in the ultraviolet region is 30,000 sec; for the visible region it is 0.25 sec; and for the IR region it is 10 sec (1). On the basis of these findings, the visible region has the potential to cause the most damage in the

least amount of time for continuous-wave lasers.

The majority of laser safety studies have been conducted at wavelengths in the visible spectrum (0.4 to 1.4 μm) because the laser energy is absorbed almost completely by the retina. The retina has a limited capacity to regenerate and repair after damage; therefore, any damage to the retina may lead to permanent visual acuity loss (19). Some examples of lasers that operate in the visible spectrum are laser pointers, compact disc readers, and barcode readers. In medicine (dermatology), ruby lasers are used for hair removal and to treat tattoos and pigmented lesions.

Lasers operating in the IR region have not been studied as thoroughly as lasers in the visible region (4, 5, 11, 19, 24). The primary target for IR laser energy absorption is the cornea which, unlike the retina, has the capacity to regenerate or repair itself. Because the cornea accomplishes about 85% of the focusing in the eye, a change in corneal shape or transparency can have a pronounced effect on vision (11, 20, 24). The cornea also is highly innervated. Accordingly, even limited damage can still cause marked pain and dysfunction (21). Prior to the advent of lasers, the primary concern for IR radiation exposures were high-temperature sources, such as welding (19, 20, 22, 27). With the advent of more modern IR laser systems (e.g., remote thermal detectors, thermal imagers, range finders, and communications devices), the IR exposure potential is enhanced greatly. In addition, current medical technologies are replete with exposure potential. For example, the CO₂ laser is an important tool in surgery for both cutting and cauterization of tissues. Yttrium aluminum garnet (YAG) lasers are used for cutting and cauterization, as well as for tissue ablation and hair removal. Because the effects of laser energies in the IR region have not been thoroughly studied, current safety standards for this region have been extrapolated from study results done at 10 μm (1). Further research on thresholds to validate or update these extrapolations is necessary.

We chose to test an IR wavelength of 3.8 μm for several reasons. The bulk of the studies that have been conducted in the IR region have been at its extremes, focusing around 1.4 and 10.0 μm . There have only been a few studies of the mid-infrared region (4, 15), which are summarized in Table 1. Water absorption is thought to be the key factor in determining the type and extent of damage to the cornea from laser energy in the IR region. However, it is

Received: 5/24/05. Revision requested: 9/23/05. Accepted: 10/01/05.
Uniformed Services University of the Health Sciences, Department of Preventive Medicine and Biometrics, Bethesda, Maryland¹; Colorado State University, Department of Environmental and Radiological Health Sciences, Fort Collins Colorado².

*Corresponding author.

Table 1. Summary of cornea studies using laser wavelengths of ~3.8 μm

Wavelength (μm)	Pulse duration	ED ₅₀ ^a (J cm ⁻²)	Spot size	Model	Reference
3.731	500 msec	7.09	0.72 mm ²	rhesus monkey	4
3.698	125 msec	4.61	0.72 mm ²	rhesus monkey	4
2.900	100 nsec	6.99	2.0 cm ²	rabbit	15
2.795	500 msec	4.72	0.53 mm ²	rhesus monkey	4

^aED₅₀ is the estimated dose at which 50% of the exposure trials result in a given response. In the case of cornea safety studies, this response is the presence of a superficial gray or white spot resulting from the laser exposure.

well known that water absorption varies by two orders of magnitude (13.7 to 667 cm⁻¹) in the IR range (11). In addition, water absorption in the IR region has several maxima and minima, with one minimum at approximately 3.8 μm (132 cm⁻¹; 8), as illustrated in Fig. 1. As the absorption coefficient increases, the depth of penetration decreases. The highest absorption coefficients theoretically result in more energy being deposited in a thinner layer of tissue, leading to more thermal damage than would be associated with smaller absorption coefficients. Therefore, 3.8 μm is an appropriate starting point to determine whether safety standards in place are protective.

The current method of corneal research, the live-rabbit model, is costly and time-consuming. Although live-animal research is still considered the most reliable and reproducible way of simulating a human response, logistical support and cost often can be prohibitive. Accordingly, it would be beneficial if the number of live animals used during testing could be reduced to only those required to verify the results supported by other models.

We chose the ex vivo pig eye as a model system because it is a readily available organ and is relatively inexpensive compared with ex vivo rabbit and rhesus monkey tissues. In addition, the pig eye is slightly larger than the rabbit eye, so more area is available for corneal investigations. The ex vivo pig eye is used frequently for mechanical stress tests and for laser eye surgery studies because of its comparability to the human eye; however no data have been established for the use of the ex vivo pig eye in laser safety studies (2, 9, 16, 17, 18, 23).

There have been some attempts in the past to evaluate replacement models for the live rabbit in laser safety studies. Some of these models include ex vivo rabbit eyes and corneal equivalent tissue cultures (7, 12, 13). The use of ex vivo tissue is a reasonable alternative to live animals for many reasons. First, if properly harvested and preserved, the complex structure of the ocular globe can be maintained. If the globe and cornea can be maintained, the initial damage to the tissue from a laser pulse can be determined. With more robust preservation techniques, it may be possible to examine tissue and corneal healing processes. However, dissipation of heat and other physiologic functions inherent in the live-animal model would not be readily apparent. Second, because the tissue is from animals euthanized for other reasons, the ex vivo model minimizes the number of animals needed for a given experiment. Third, the use of ex vivo tissue does not require a veterinarian or other highly trained individual to administer anesthesia, pain management, or postprocedural care. Finally, the avoidance of animal protocols saves time and money, allowing for more rapid performance of experiments with fewer external requirements. Although corneal equivalent tissue culture appears to be a promising alternative to the live-animal model, many of the benefits of the ex vivo eye are not present with the corneal equivalent (7). Tissue culture is both time- and

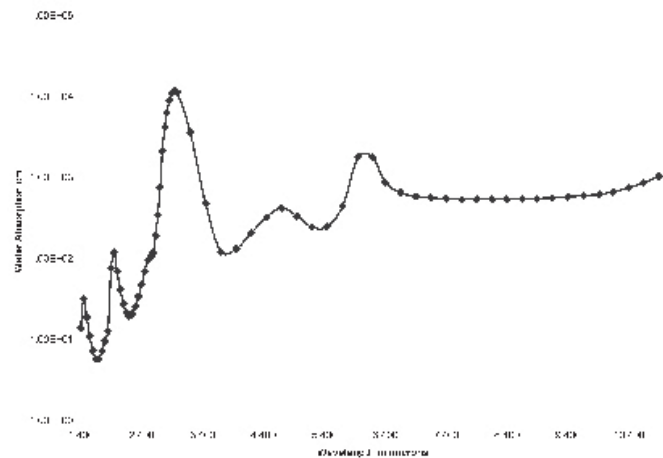


Figure 1. Absorption coefficients associated with water for wavelengths of photonic energy ranging from 1.4 to 10.4 μm (the infrared spectrum).

resource-intensive and requires special knowledge and training. The purpose of the present study was to evaluate the viability of ex vivo pig eyes as a replacement model for in vivo testing in the establishment of laser eye safety standards.

Materials and Methods

Eye preparation. A total of 24 eyes were enucleated from 12 healthy pigs: five 4- to 6-month-old Yucatan mini-pigs (Sinclair Research Inc., Auxvasse, Mo.) and nineteen 5- to 6-month-old Yorkshire pigs (Charles River PharmServices, Southbridge, Mass.). These animals were not euthanized solely for this experiment but were used previously in other protocols approved by the Uniformed Services University for the Health Sciences. All animals were cared for in accordance with guidelines from the Association for the Assessment and Accreditation of Laboratory Animal Care, International. The eyes were obtained under a tissue-sharing protocol. Animals were acclimated for 2 weeks prior to euthanasia. Animals were euthanized with Buthanasia-D Special (Schering-Plough, Union, N.J.) at 1 mL/10 kg intravenously while they were under general anesthesia. Immediately upon euthanasia of each animal (within minutes), eyes were collected with clean instruments in a sterile location and by using methodology designed to minimize the possibility of biological contamination (i.e., by using latex gloves, changing gloves and cleaning instruments between animals, etc.). The eyes were removed, rinsed with saline, and placed directly in Dulbecco's Modified Eagle Medium with 10% fetal bovine serum (Invitrogen, Carlsbad, Calif.) and then placed in 3 to 10% CO₂ bags (GasPak EZ 260684, Becton Dickinson, Sparks, Md.) and refrigerated at ~10°C. Refrigeration was important to minimize the growth of biological contaminants and preserve tissue integrity.

The eyes were stored 24 to 48 h before being exposed to laser radiation. Before laser exposure, the eyes were brought to room temperature (~20°C) over a period of approximately 30 min, washed in excess 0.9% saline, and placed on gauze supports. An identification marker was made with the date and exposure number written in pencil on a slip of paper. The use of pencil was important as pen ink dissolved in formalin, which was the preservation solution. Prior to exposure, the eye was photographed with the identification marker and placed on an exposure platform.

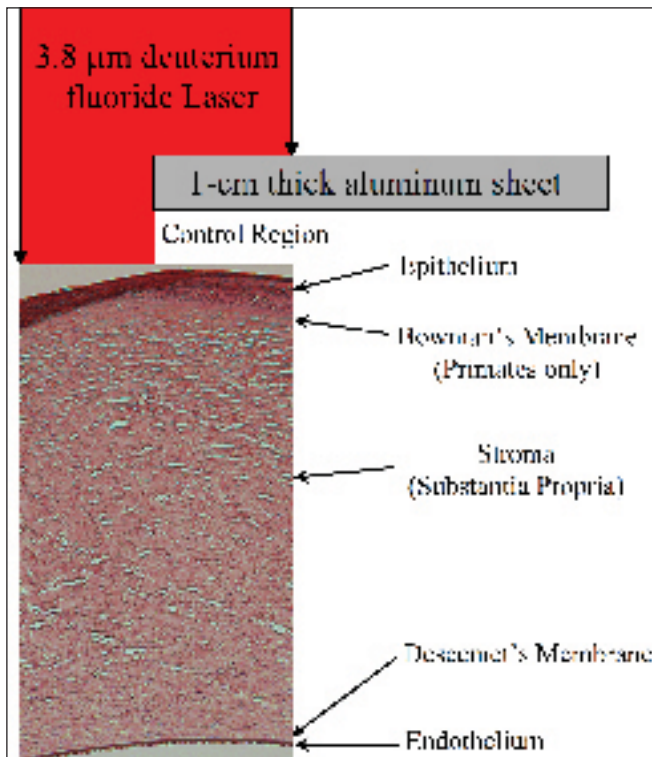


Figure 2. Pictorial cross-section representing the site of laser interaction with the porcine cornea. Cell layers of the porcine cornea are labeled. Note that the porcine cornea does not have a Bowman's membrane. Its location in the primate cornea is indicated for reference purposes only.

Laser exposure. Once the eye was positioned with the pupil oriented upward, a 1-cm thick sheet of aluminum was placed horizontally over half of the eye to create a control region. The eye was then wet with 1 to 2 mL 0.9% saline solution approximately 20 sec prior to the laser exposure. The detail of the experimental setup is shown in Fig. 2.

The laser used for all exposures was a 3.8- μm deuterium fluoride chemical laser with a square, 'top-hat' (uniform energy density) profile, a pulse width of 8.0 μs , and a spot size of 4 cm^2 . The spot size was precisely measured at the beginning and end of each experimental day by exposing Kodak T- Mat G Film (part number 1373125, Eastman Kodak Co., Rochester, N.Y.) to the laser pulse. The exposed film then was measured using a micrometer to determine the area of the spot. During each exposure, fluence and total energy were measured using a Gentec ED-500 LIR plus (Gentec Electro-Optics, Inc., Québec, Canada) and recorded. Instruments are calibrated annually with NIST traceable standards. Each eye was exposed to a single 8.0- μs pulse, and the exposures delivered to the tissue samples ranged from 4.0 J to 31.8 J cm^{-2} .

After exposure to the laser, three different observers determined whether there was any damage to the eye. The criterion used for minimal damage was identical to that used by Brownell and Stuck (3), namely, the presence of a superficial gray-white spot that develops within 30 min of the exposure. Once a consensus between the observers on the presence or absence of damage was reached, photographs of the eye were obtained. Each observer was trained in at least two previous studies on identification

of changes to the cornea and evaluated the eye independently prior to obtaining any information on the fluence. The eye was wrapped with the identification marker in gauze immediately after completion of evaluation and photographs and placed in 10% buffered formalin for preservation.

Postexposure. After exposure, the eyes were prepared for histological evaluation after a minimum of 48 h in formalin. The eyes were blocked in paraffin, cut in sagittal sections (epithelial to endothelial surfaces) to a thickness of 8 μm , stained with hematoxylin and eosin, and mounted on a glass slide. Each cornea was completely photographed using a Leica Microsystems microscope with digital camera attachment in conjunction with QCapture software (version 1.68.6, Quantitative Imaging Corporation, Burnaby, Canada). Each photographed section was digitally measured using Image ProDiscovery software (Media Cybernetics, Inc., Silver Spring, Md.). In those areas of the cornea where vacuoles formed (most likely secondary to steam propagation), measurements were obtained from the base of the vacuole to the deepest layer of the cornea or endothelium. In areas where no vacuole formation was present, such as control regions, measurements were taken from the outer epithelium to the endothelium (i.e., the total corneal thickness). Measurements were made every 100 μm across the width of the cornea with approximately 7000 total measurements taken. Depth of penetration measurements were not used for statistical analysis but were taken to evaluate the tissue response against the expected outcome based upon safety standards set by ANSI. These results will be presented in a future publication.

Statistical analysis. Each cornea was examined visually immediately (within 1 min) postexposure for any abnormalities or indications of gross morphologic changes. Each exposed cornea then was coded based upon a binary code (0, no damage; 1, damage). Analysis of the gross response of the tissue was performed using probit statistics because of the binary nature of the data and its stochastic response. The estimated dose 50 (ED_{50}), where 50% of the trials are expected to result in a given effect, is the statistical standard used by ANSI in the establishment of safety standards (1). The program EZ Probit was used to calculate the ED_{50} (6). Only the initial gross morphological examination was used for statistical analysis.

Results

Gross morphology. Immediately after exposure (within 1 min), the eyes were classified as either damaged (clouding present in the cornea) or undamaged (no corneal clouding observable). At higher energies, the observed damage included pitting and ablation of the cornea extending to the stromal layer. The general trend of increasing damage correlating with increasing fluence can be seen in Fig. 3. One point of particular interest is at 9.9 J cm^{-2} . Until that point, damage to the cornea increased with increasing fluence. At 10.3 J cm^{-2} there seemed to be a decrease in corneal damage, which then gradually intensified with further increases in fluence. This damage plateau observation is further validated by the histology, which shows that the depth of penetration decreased at this point. Indeed, the mechanism of damage appeared to change as well.

An analysis of the gross response of the cornea indicated an ED_{50} of 6.7 J cm^{-2} (with a slope of 31.9 and a chi-square probability of 0.9977). There was a negative response at 7.0 J cm^{-2} and a positive response at 6.6 J cm^{-2} . The gross response of the corneas

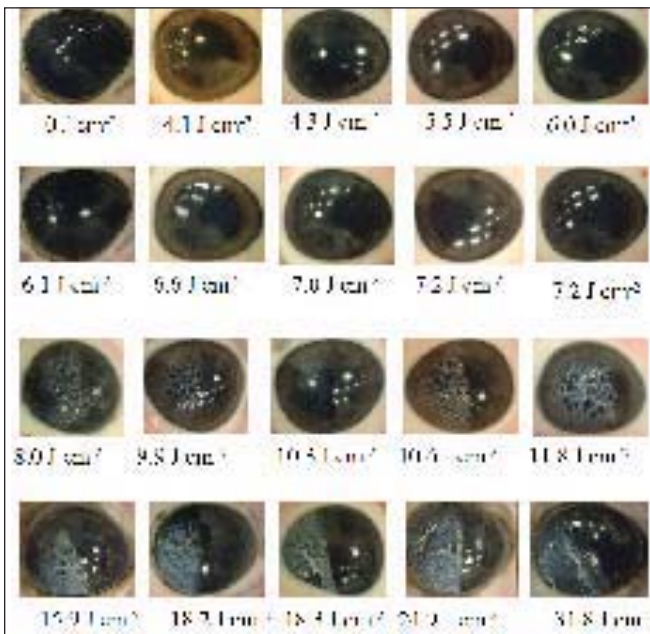


Figure 3. Gross corneal damage immediately after exposure at increasing fluence (in $J\ cm^{-2}$).

were almost deterministic, with the exception of this one data point. Fiducial limits could not be calculated using this data set.

Histology. There are three regions of interest in the data regarding changes to the cornea and depth measurements (Fig. 4). Region A contains the two lowest energies (4.09 and $4.3\ J\ cm^{-2}$) and yielded a negative depth measurement, indicating swelling in the epithelial layer of the exposed region. Region B ranges from 5.5 to $9.9\ J\ cm^{-2}$ and showed linear increasing depth of damage, with an exponential component at the upper end. Region C includes all fluences $> 9.9\ J\ cm^{-2}$, which were associated with a dramatic drop in radiation penetration depth followed by a general upward linear trend with wide variation.

Region A includes fluences of 4.1 and $4.3\ J\ cm^{-2}$. In this region, the cornea showed no gross damage just prior to exposure, after which there was an observable ridge running down the center of the cornea. It was first assumed that this ridge was a corneal abnormality that was missed prior to exposure; however, a subsequent exposure yielded the same result. In fact, tissue histology revealed swelling in the epithelial layer (Fig. 5B) when compared with the control region (Fig. 5A). It was not possible to measure depth of laser radiation penetration because there was no definable cellular damage beyond the swelling, which averaged approximately $20\ \mu m$. It was clear that energy absorption caused change, but it was difficult to quantify because there was no vacuolization.

The next region of interest was Region B, with fluences from $5.5\ J$ to $9.9\ J\ cm^{-2}$. Histologic evaluation demonstrated limited cellular damage that was contained to the epithelium. It was characterized by vacuolization, slight nuclear condensation, and cellular swelling (Fig. 5C). In both regions A and B, the damage seemed to be localized in one layer, with all damage at the depth of penetration and leaving the tissue which the laser radiation passed through unchanged.

The last region of interest was Region C, with fluences $> 9.9\ J\ cm^{-2}$. The average penetration at the center of the cornea was

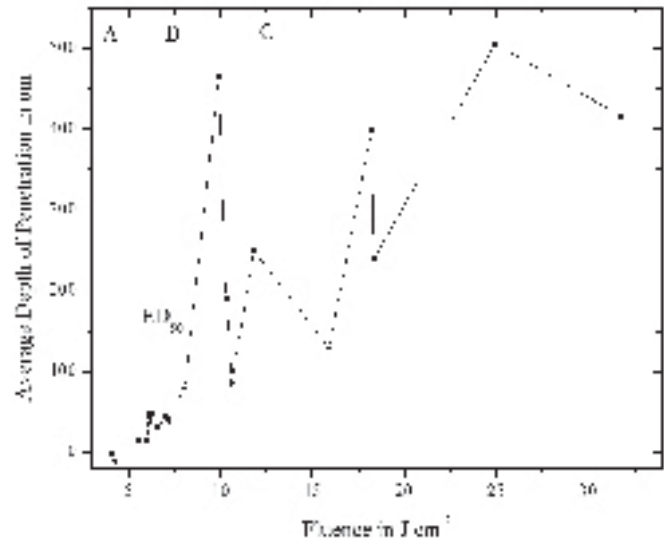


Figure 4. Graphical representation of the average depth of laser radiation penetration of the porcine cornea versus incident fluence. Exposures in Region A were associated with evidence of swelling of the epithelial layer. Exposures in Region B led to direct correlation between the incident fluence and the depth of penetration. Region C showed a great amount of variability.

$129\ \mu m$. Tissue evaluation revealed extensive cellular damage in the epithelial layer and vacuole formation in the substantia propria (stroma; Fig. 5D). Damage to the epithelial layer was characterized by vacuolization (steam generation), cellular deformation, nuclear condensation, and cellular destruction and swelling. The primary mechanism of damage appeared to be marked surface heating. Damage to the stromal layer was characterized by vacuolization, nuclear condensation, and cellular destruction. Further, the damage to the stromal layer was not uniform: in some locations, there was no evidence of laser radiation penetration past the epithelium, whereas in others, the damage extended from a few micrometers to $> 100\ \mu m$ into the stroma. In addition, the overall mechanism of damage seems to be different in Region C compared with those of Regions A and B. The damage in Region C appears to be due to pronounced heat generation on the surface, which extends completely through the corneal tissue. Tissue damage in Region C was not as localized as it was in Region B.

Discussion

There are several unique aspects of our study that materially differ from those of other similar efforts. These aspects include the wavelength of interest, the large spot size of the laser, and the use of the ex vivo pig eye.

It has been previously noted that for IR lasers, the threshold for gross morphologic changes is dependent on spot size up to a specific area (25). Past studies at $3.8\ \mu m$ used a 1.1-mm circular spot size, which may be difficult to evaluate visually (4). A spot size of $4\ cm^2$ was chosen for this study to avoid spot-size-dependency issues and to facilitate identification of gross changes to the cornea. Our use of a large laser spot for this study ($4\ cm^2$) may have been an important factor in the repeatability of the response from eye to eye.

During the design of the experiment we considered exposing the eyes at $37^\circ C$, but the logistics of performing the exposures at $37^\circ C$ when considering optics and the laser operation were

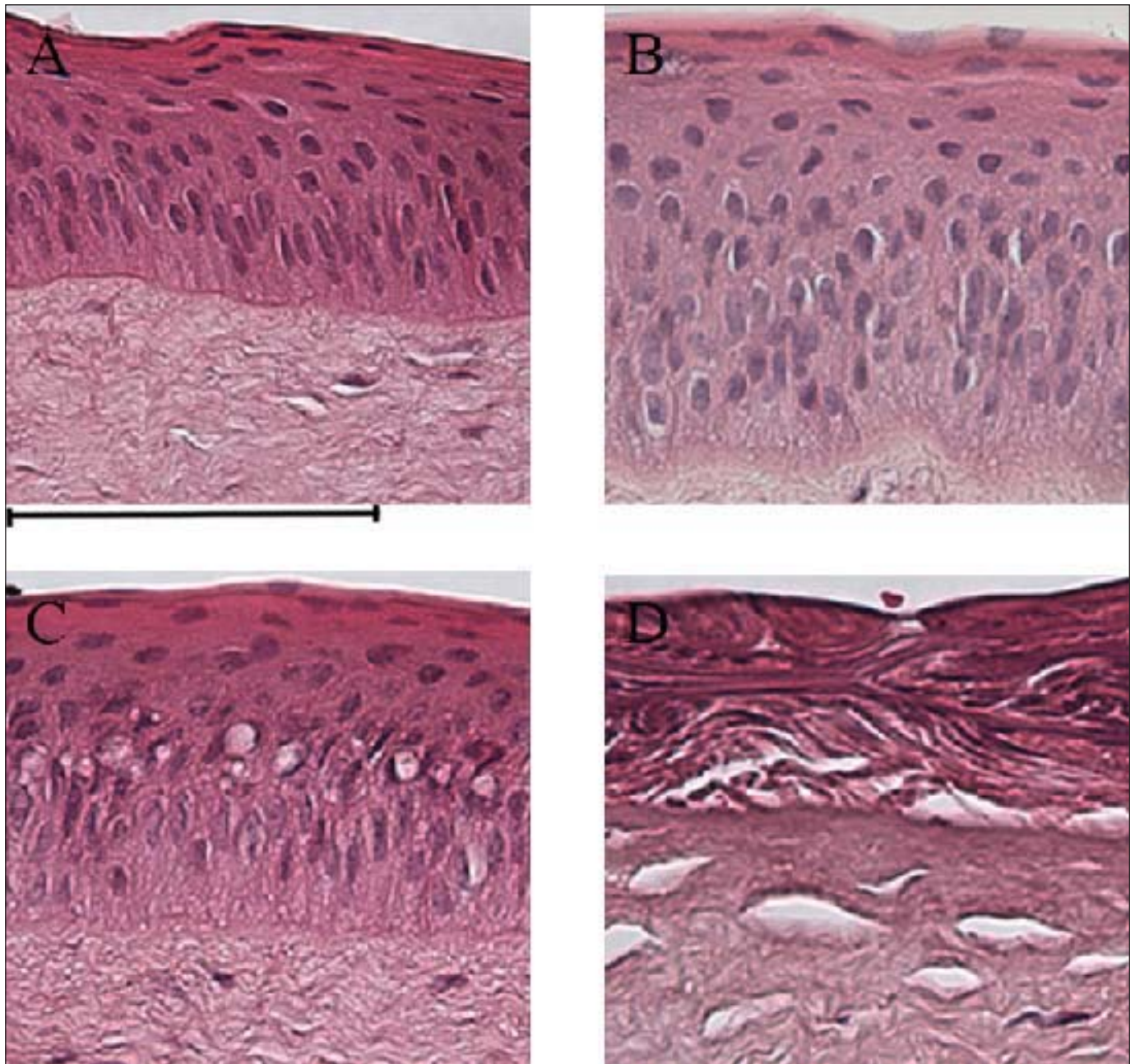


Figure 5. Representative histologic sections of cornea (H&E stain; magnification, $\times 200$). (A) Unexposed control. (B) Region A; sample shown was exposed at 4.3 J cm^{-2} . Cellular swelling evident, but no other identifiable damage. (C) Region B; sample shown was exposed at 6.59 J cm^{-2} . Vacuole formation within the epithelial layer. (D) Region C; sample shown was exposed at 15.90 J cm^{-2} . Extensive cellular damage extending into the stroma. Bar is 100μ . $\times 20$ objective.

overwhelming. In addition, the change in temperature from 10 to 37°C and then back to room temperature after exposure was thought to produce more of an environmental shock than that of a graded change to room temperature. This shock might have introduced changes that were not predictable.

The last parameter that must be addressed is the comparability of the pig cornea to the human cornea and the two most frequently used models, namely the rabbit eye and rhesus monkey eye. For the purposes of laser safety studies, the most pertinent aspects of these models have been summarized in Table 2 (10, 14,

23). The results of our study seem to show that the ex vivo pig eye is a suitable model for evaluation of laser safety standards. The range of exposures studied (4.0 to 31.8 J cm^{-2}) was selected to span from the threshold for a minimally visible lesion to a point where damage appeared to plateau. The resulting ED_{50} of 6.7 J cm^{-2} compared very well with previous studies (Table 1) and supports the use of pig eyes as a useful model for evaluating threshold gross morphologic changes.

Approximately 7000 data points were collected while measuring corneal damage and subsequently graphed (Fig. 6). This

Table 2. Comparison of pertinent aspects of the corneas of the pig, human, and rabbit models

Model	Globe diameter (mm)	Corneal thickness (μm)	Corneal epithelium thickness (μm)	Bowman's membrane present?
Human	24	770	35	yes
Rhesus monkey	20	460	30	yes
Rabbit	18	450	30	no
Pig	30	1063	47	no

graph is a three-dimensional model representing all depths of damage at all fluences and illustrates the advantage of using the ex vivo pig eye over most other frequently used animal models. Two regions of interest are noted in different colored bands. The region above the yellow band represents the overall thickness of the rhesus monkey and rabbit corneas. The region above the black band represents the overall thickness of the human corneal. This information implies that points recorded below these bands corresponds to laser radiation that might have passed through the respective corneas. Therefore, potentially damaging levels of radiation might have gone unnoticed if these models had been used. Furthermore, radiation that would pass through the human cornea, possibly causing damage to the retina or lens, was captured and quantified in our pig cornea model. This attribute makes it possible to calculate the amount of energy that would be transmitted through the human cornea to determine whether damaging levels of radiation would reach the lens or retina.

Our study had some limitations due to the time constraints caused by the availability of the laser system. A slit-lamp was not used to determine the presence of corneal damage; if it had been, our damage threshold may have been lower than that observed. In addition, the spot size we used was approximately two orders of magnitude greater than that typically used in past laser safety studies, and this increased spot size affected the thermal distribution and uniformity of energy incident on the cornea.

Additional studies are necessary to ascertain whether the results from the thicker pig cornea could be modeled in conjunction with those from rabbit cornea. Because the pig cornea is thicker than that in humans and the rabbit cornea thinner than that in humans, it is possible that an average or a constant could be applied to better approximate the human cornea. An ex vivo rabbit eye study at this wavelength would make a good starting point to identify modeling prospects to address this issue.

Despite these limitations, this study suggests the ex vivo pig eye is a potential replacement model for live animals. The histology presented in a manner consistent with thermal damage as expected, and the ED₅₀ was well within statistical limits of other exposures at this wavelength. Overall, the tissue response was consistent with what would be expected in an in vivo model. Further experimentation is necessary to confirm the utility of this model over others; however, it seems clear that the use of ex vivo pig eyes could reduce the number of live animals needed to establish safety standards. Indeed, at the very least, ex vivo pig eyes could be used to ascertain a dose range for in vivo studies, thus minimizing the use of animals.

Acknowledgments

The opinions or assertions contained herein are the private ones of the authors and are not to be construed as official or reflecting the views

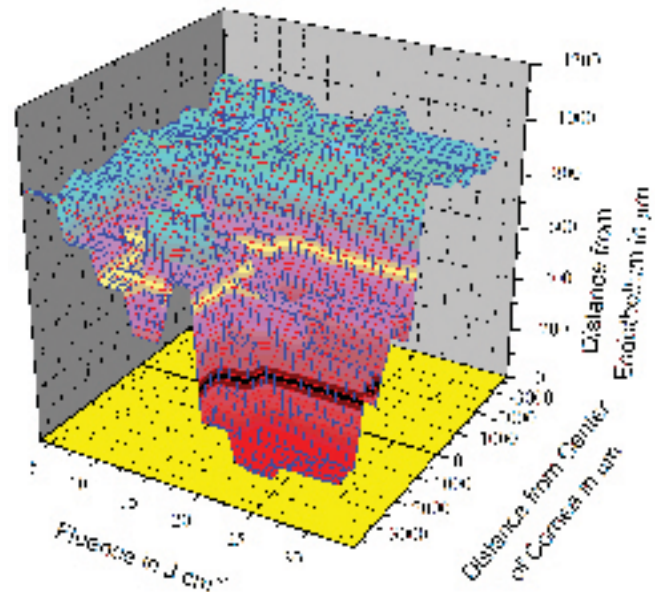


Figure 6. A three-dimensional representation of the depth of penetration across the cornea for all fluences. The correlation between increasing penetration depth and increasing fluence is evident. The yellow line represents the thickness of the rhesus monkey and rabbit corneas. The black line represents the thickness of the human cornea. Blue indicates epithelial layer thickness and red represents penetration in stroma.

of Colorado State University, the United States Department of Defense, or the Uniformed Services University of the Health Sciences. We would like to thank Don Randolph, Golda Winston, Trida Winston, and Scott Johanson for their assistance in tissue exposure and collection.

References

1. **American National Safety Institute.** 2000. American national safety standard for safe use of lasers (ANSI Z136.1-2000). Laser Institute of America, Inc., Orlando, Fla.
2. **Brinkmann R., B. Radt, C. Flamm, J. Kampmeier, N. Koop, and R. Birngruber.** 2000. Influence of temperature and time on thermally induced forces in corneal collagen and the effect on laser thermokeratoplasty. *J. Cataract Refract. Surg.* **26**:744-754.
3. **Brownell, A. S. and B. E. Stuck.** 1974. Ocular and skin hazards from CO₂ laser radiation, p. 123-138. *In Proceedings of the 9th Army Science Conference.* U.S. Military Academy, West Point, N.Y.
4. **Dunsky, I. L. and D. E. Egbert.** 1972. Corneal damage thresholds for hydrogen fluoride and deuterium fluoride chemical lasers, p. 1-28. U.S.A.F. School of Aerospace Medicine, San Antonio, Tex.
5. **Egbert, D. E. and E. F. Maher.** 1977. Corneal damage thresholds for infrared laser exposure: empirical data, model predictions, and safety standards, p. 1-61. U.S.A.F. School of Aerospace Medicine, San Antonio, Tex.
6. **Finney, D. J.** 1971. Probit analysis, 3rd ed. Cambridge University Press, Cambridge.
7. **Fletcher, D. J., T. E. Johnson, M. A. Mitchell, T. E. Eurell, P. J. Rico, and W. P. Roach.** 2000. Corneal equivalents: a replacement model for in vivo 1540 nm laser exposure studies, vol. 3907, p. 468-475. *In R. R. Anderson, K. E. Bartels, L. S. Bass, C. G. Garrett, K. W. Gregory, N. Kollias, H. Lui, R. S. Malek, G. M. Peavy, H.-D. Reidenbach, L. Reinisch, D. S. Robinson, L. P. Tate, E. A. Trowers, and T. A. Woodward (ed.), Lasers in surgery: advanced characterization, therapeutics, and systems x.* Proceedings of Society of Photo-Optical Instrumentation Engineers. Society of Photo-Optical Instrumentation Engineers, San Jose, Calif.

8. **Hale, G. M. and M. R. Querey.** 1973. Constants of water in the 200 nm to 200 μm wavelength region. *Appl. Opt.* **12(3)**:555-563.
9. **Hiroko Bissen-Miyajima, M., K. Nakamura, M. Kaido, S. Shimmura, and K. Tsubota** 2004. Role of the endothelial pump in flap adhesion after laser in-situ keratomileusis. *J. Cataract Refract. Surg.* **30**:1989-1992.
10. **International Commission on Radiological Protection 23.** 1975. Report of the task group on reference manual, p. 480. Pergamon Press, Elmsford, N.Y.
11. **Maher, E. F.** 1978. Transmission and absorption coefficients for ocular media of the rhesus monkey, p. 102. U.S.A.F. School of Aerospace Medicine, San Antonio, Tex.
12. **McCally, R. L.** 1997. Corneal damage from infrared radiation, p. 1-24. Johns Hopkins University, Laurel, Md.
13. **McCally, R. L., R. A. Farrell, and C. B. Barger.** 1992. Cornea epithelial damage thresholds in rabbits exposed to Tm:YAG laser radiation at 2.02 microns. *Lasers Surg. Med.* **12(6)**:598-603.
14. **Merindano, M. D., J. Costa, M. Canals, J. M. Potau, and D. Ruano.** 2002. A comparative study of bowman's layer in some mammals: relationships with other constituent corneal structures. *Eur. J. Anat.* **6(3)**:133-139.
15. **Mueller, H. A. and W. T. Ham, Jr.** 1976. The ocular effects of single pulses of 10.6 μm and 2.5-3.0 μm Q-switched laser radiation, p. 1-18. *In* A report to the Los Alamos scientific laboratory L-division. Department of Biophysics, Health Sciences Division, Virginia Commonwealth University, Richmond, Va.
16. **Müller, M. B., P. T. Boeck, and P. C. Hartmann.** 2004. Effect of excimer laser beam delivery and beam shaping on corneal sphericity in photo-refractive keratectomy. *J. Cataract Refract. Surg.* **30**:464-470.
17. **Seitz, B., A. Langenbacher, C. Hofmann-Rummelt, U. Schlotzer-Schrehardt, and G. O. Naumann.** 2003. Nonmechanical posterior lamellar keratoplasty using the femtosecond laser (femto-plak) for corneal endothelial decompensation. *Am. J. Ophthalmol.* **136(4)**:769-772.
18. **Seitz, B., H. Brunner, A. Viestenz, C. Hofmann-Rummelt, U. Schlotzer-Schrehardt, G. O. Naumann, and A. Langenbacher.** 2004. Inverse mushroom-shaped nonmechanical penetrating keratoplasty using a femtosecond laser. *Am. J. Ophthalmol.* **139(5)**:941-944.
19. **Sliney, D. H.** 1983. Biohazards of ultraviolet, visible and infrared radiation. *J. Occup. Med.* **25(3)**:203-210.
20. **Sliney, D. H.** 1993. Infrared laser effects on the eye: implications for safety and medical applications. *In* Laser applications. The International Society for Optical Engineering, Bellingham, Wash.
21. **Sliney, D. H., J. Mellerio, V. P. Gabel, and K. Schulmeister.** 2002. What is the meaning of threshold in laser injury experiments? Implications for human exposure limits. *Health Phys.* **82(3)**:335-347.
22. **Sliney, D. H., K. W. Vorpahl, and D. C. Winburn.** 1975. Environmental health hazards from high-powered, infrared, laser devices. *Arch. Environ. Health* **30(4)**:174-179.
23. **Svaldeniene, E., V. Babrauskienė, and M. Paunksniene.** 2003. Structural features of the cornea: light and electron microscopy. *Veterinarija Ir Zootechnika* **24(46)**:50-55.
24. **Takata, A. N., L. Goldfinch, J. K. Hinds, L.B. Kuan, N. Thomopoulos, and A. Wiegandt.** 1974. Thermal model of laser-induced eye damage. IIT Research Institute, Chicago.
25. **Thomas, J. J., C.P. Cain, D. J. Stolarski, K. J. Schuster, T.A. Eggleston, G. D. Noojin, K. Stockton, and W. P. Roach.** 2003. Comparative analysis of spot size dependence for lesions produced by infrared laser pulses, vol. 4953, p. 124-130. *In* B. E. Stuck and M. Belkin (ed.), Laser and noncoherent light ocular effects: epidemiology, prevention, and treatment. Proceedings of Society of Photo-Optical Instrumentation Engineers. Society of Photo-Optical Instrumentation Engineers, San Jose, Calif.
26. **Vogel, A. and V. Venugopalan.** 2003. Mechanisms of pulsed laser ablation of biological tissues. *Chem. Rev.* **103(2)**:577-644.
27. **Wolbarsht, M.** 1980. Damage to the lens from infrared. *In* Ocular effects of non-ionizing radiation. The Society of Photo-Optical Instrumentation Engineers, Washington, D.C.